Sports Engineering (2024) 27:20
https://doi.org/10.1007/s12283-024-00462-8

ORIGINAL ARTICLE

Leg stiffness and energy minimisation in human running gaits

Zofia Wróblewska[1] · **Piotr Kowalczyk**[1] · **Krzysztof Przednowek**[2]

Accepted: 7 May 2024 / Published online: 18 June 2024

Abstract
A novel application of spring-loaded inverted pendulum model is proposed in this study. In particular, we use this model to find the existence of so-called fixed points, which correspond to actual running gaits, as functions of model parameters such as stiffness and energy. Applying the model to experimental data allows us to draw justifiable conclusions on mechanical energy minimisation for running gaits. The data were collected during a study witch 105 athletes. Force was measured using a pressure plate integrated in a treadmill. Kinematic data were recorded using two high-speed video cameras and an accelerometer placed on the back sacral localization. Each athlete completed trials by running at four different targeted velocities (9, 12.5, 16, 19.5 km/h). Running velocity influenced the values of the leg spring stiffness approximations, while the values of stiffness, determined using data from the pressure plate and camera, vary only slightly. The mechanical energy corresponding to periodic running gaits was studied with leg stiffness determined from the experiment. The mechanical energy of the runner slightly exceeded the minimum value of energy required for the existence of fixed points in the model. These results contribute to the general understanding of running gaits in terms of mechanical energy optimization.

Keywords Spring-mass model · Running gaits · Approximate solutions · Model verification · Practical calculation

1 Introduction

The correlation between human movement patterns and running economy is widely acknowledged, cf. [1, 2]. These connections are multifaceted, and unraveling their complexities can prove to be an invaluable pursuit in the realm of sport science. For example, it is assumed that reduced variability of key biomechanical parameters such as vertical oscillations is crucial to athletic performance [3]. Current research primarily focuses, either, on experimental data analysis [4–7], or on mainly theoretical investigations of the behavior of a mathematical model over time, see [8–14]. To provide a comprehensive assessment of the mechanics and energetics of the running gait, this study utilizes a combination of experimental data analysis and mathematical modeling. In this way our research fills an important gap in that the model is used as a reference for measured mechanical parameters, and it also allows for an assessment of mechanical optimization of running. Model parameters such as stiffness and mechanical energy are determined from experimentally collected human running data. By utilizing the existing deterministic model and its approximate analytical solutions [15], experimentally determined parameter values are compared with the constraints deduced from the theoretical studies of the model.

The mechanical behavior of the lower limbs' musculoskeletal system while running is frequently compared to that of a spring-mass system bouncing into the ground during the so-called support phase, which is followed by the flight phase. This simple model, consisting of a spring-loaded inverted pendulum (later termed as SLIP model) was first proposed in [16, 17]. The main mechanical parameter which has been most widely studied in various papers [17–24] is the stiffness of the leg. It characterizes the elastic behavior

Piotr Kowalczyk and Krzysztof Przednowek contributed equally to this work.

✉ Zofia Wróblewska
zofia.wroblewska@pwr.edu.pl

Piotr Kowalczyk
piotr.s.kowalczyk@pwr.edu.pl

Krzysztof Przednowek
krprzednowek@ur.edu.pl

[1] Department of Mathematics, Wrocław University of Science and Technology, Wybrzeże Wyspiańskiego 27, 50-372 Wrocław, Poland

[2] Institute of Physical Culture Sciences, University of Rzeszów, mjr. Kopisto 2a, 35-959 Rzeszow, Poland

of the leg in the model, and it is determined by the relationship between its deformation and the force applied to it. (Strictly speaking the stiffness parameter introduced in the model measures the stiffness of the whole body.) Leg spring stiffness also appears in the equations of motion, and so it is necessary for obtaining the center of mass trajectory. By observing the vertical position of a point mass and its changing velocity, the system's mechanical energy can be calculated and taken as the basis of the overall mechanical approach. According to our previous research, the appropriate energy of the system, which depends on the set angle of attack and angular velocity at touch-down, is one of the mechanisms ensuring the motion's stability [15].

The main aim of this study is to investigate the optimization of mechanical energy during running. To the best of our knowledge, there has not been reported in the literature the use of reduced SLIP model as a reference which allows one to determine optimization of running mechanical energy. To do so, a given value of measured mechanical energy is compared with the minimum energy required for stable running as predicted by the model. By feeding into the model specific parameters such as: the vertical and horizontal velocity, the angle of attack, and energy, a comparison between the analytically determined values of stiffness with experimentally gathered data was performed. Thanks to this, we verified whether the order of magnitude of the real data was consistent with the results returned by the model. In this way, we validated the predictive power of SLIP model. We then selected an appropriate approximation order of the stiffness parameter for further analysis. Furthermore, we evaluated the approximation of contact time of the foot with the ground, leg deflection, and the difference between the attack and take-off angles during the stance phase.

The SLIP model which we use is both a limitation and a strength. That is, the analysis which allowed us to reduce the mechanics to a one-dimensional problem gives us a possibility of straightforward comparison of the energetics with a given reference provided by the model. However, the particulars of running such as, for example, the effects on the stiffness parameter of particular parts of the lower limbs during running is lost in the modeling process.

2 Materials and methods

2.1 Spring-mass running model

2.1.1 Model statement

It is known that the spring-mass model of running assumes that each leg in the stance phase can be described as an inverted elastic pendulum (cf. [12, 15–17, 25]). We assume a situation depicted in Fig. 1.

Below is the mathematical description of this model during the contact phase (see (1)). We use nondimensional, depending on time, polar coordinates (L, θ) for the point mass m. Assuming a small angle θ, between the leg and vertical axis, we can write

$$\begin{cases} L\theta'' + 2L'\theta' = \sin\theta, \\ L'' - L(\theta')^2 = K(1-L) - \cos\theta. \end{cases} \tag{1}$$

The nondimensional spring length L is introduced after a division by distance l_0, which is the distance of the point

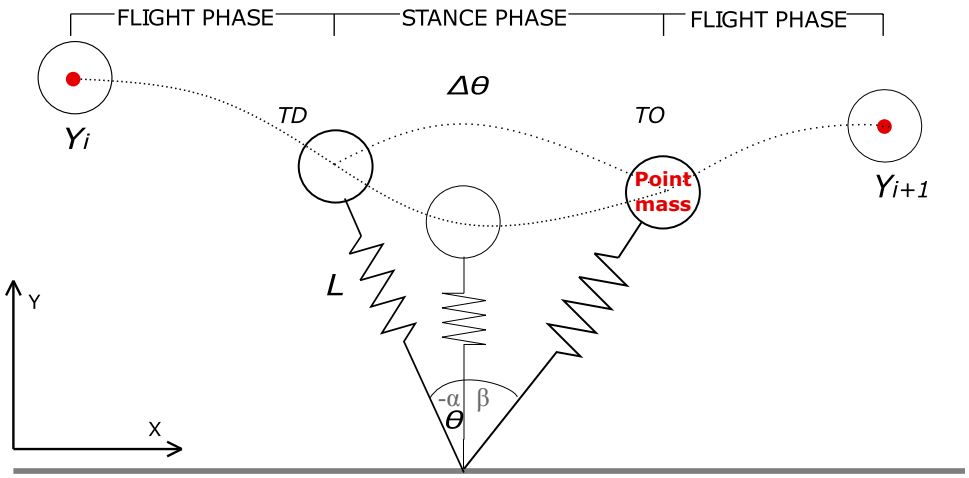

Fig. 1 The diagram illustrates a planar spring-mass model for running, in which a point mass is connected to a massless spring. The model uses dimensionless Cartesian coordinates (X, Y) and dimensionless polar coordinates (L, θ), where L represents the radial position and θ represents the angular position. The angle swept during the stance phase is represented by $\Delta\theta$. At the points of touch-down and take-off, denoted by TD and TO respectively, the angular position is $\theta_{TD} = -\alpha$ and $\theta_{TO} = \beta$, respectively, where $\alpha, \beta \in (0, \pi/2)$. The value of the radial position at each phase transition is $L_{TD} = L_{TO} = 1$. In each period, the apex height Y_i transitions to Y_{i+1}

mass from the place where the leg is in contact with the ground. The nondimensional spring stiffness present in Eq. (1) is given by

$$K = \frac{kl_0}{mg}, \tag{2}$$

where k is the dimensional equivalent of leg stiffness K, and K is the only constant in system (1). The spring stiffness K has to be determined to ensure that during the support phase the spring will return to the equilibrium length precisely at the time when the pendulum travels to the angle β. The leg completes the full support cycle before jumping into the aerial phase (see Fig. 1).

The initial conditions for the polar coordinate system have the form

$$\theta(0) = -\alpha, \quad \theta'(0) = \theta_d, \quad L(0) = 1, \quad L'(0) = -L_d, \tag{3}$$

with

$$\theta_d = U\cos\alpha - V\sin\alpha, \quad L_d = U\sin\alpha + V\cos\alpha, \tag{4}$$

where we have defined the horizontal and vertical velocities at the moment of touch-down (Froude numbers denoted by U and V).

In Table 1, we have collected all the parameters, both nondimensional and dimensional, appearing in the running model.

Proper running with constant velocity, is combined with touching-down under the center of mass, which reduces deceleration and guarantees small values of α. On the other hand, large β angles ensure that the propulsion is optimized. The β angles are clearly larger than the α angles, implying an asymmetric run.

For small angles of attack α, the angular velocity at touch-down θ_d refers to U ($\theta_d \approx U$). Therefore, the θ_d parameter range shown in Table 1 are close to U. It reflects a typical human running speed, which for one meter long legs means a jogging speed of about 3.13 m/s. Typical values of K_{real} range from around 12 to around 50 (see Table 1), where the dimensional stiffness of the leg denoted by k_{real} is defined as the ratio of the maximum force to the maximum leg compression of the leg (see (16)) and further scaled according to the formula (2). We see that in general K_{real} assumes much higher values in relation to the rest of the parameters, especially for a realistic regime of constants.

2.1.2 Approximate solutions

An asymptotic analysis of the main equations (1) with the use of the Poincaré–Lindstedt series was carried out in [21]. The solution of the system (1) is based on the perturbative expansion related to the significant spring stiffness ($K \to \infty$). Using the initial conditions (3), we obtain the approximations for $L(T)$ and $\theta(T)$ [21]. First, the time T has been made dimensionless by multiplying by the group $(g/l_0)^{1/2}$. Second, since the solutions $L(T)$ and $\theta(T)$ live on fast $\sqrt{K}T = \epsilon^{-1}T$ time scale with $\epsilon = 1/\sqrt{K}$ ($\epsilon \to 0^+$), the frequency of the pendulum formed by hanging a mass on the unstretched leg is given by $\epsilon^{-1}\widetilde{\omega}(\epsilon)$ and $\widetilde{\omega}(\epsilon) = 1 - \frac{1}{2}\epsilon^2\theta_d^2$.

For the sake of order, we will list below the successive approximations of the running parameters that were derived from $L(T)$ and $\theta(T)$ approximations in [15]. In $L(T)$, the parameter T ranges from 0 to the contact time T_c given by

$$T_c \approx \widetilde{T}_c := \frac{2\epsilon}{\widetilde{\omega}(\epsilon)} \arccos\frac{A(\epsilon)}{B(\epsilon)}, \tag{5}$$

where

$$A(\epsilon) = \epsilon^2\left(\theta_d^2 - \cos\alpha\right) \quad \text{and} \quad B(\epsilon) = \epsilon\sqrt{\epsilon^2(\theta_d^2 - \cos\alpha)^2 + L_d^2}. \tag{6}$$

Observe that $L(0) = L(T_c) = 1$ and $L(T_c/2) = 1 - \Delta L_{\max}$ (see Fig. 2 from [15]). The maximum leg deflection during stance phase, denoted by $\Delta L_{\max}$, is approximated by the difference

Table 1 Typical values of all appearing nondimensional and dimensional physical parameters

Symbol	Description	Nondimensional value	Dimensional value
α	Angle of attack ($\alpha \times 180°/\pi$)	0.03–0.31	2°–18°
β	Angle of take-off ($\beta \times 180°/\pi$)	0.31–0.61	18°–35°
U, u	Horizontal Froude number ($U \times \sqrt{gl_0}$)	0.63–1.73	2–5.5 m/s
V, v	Vertical Froude number ($V \times \sqrt{gl_0}$)	0.03–0.22	0.1–0.7 m/s
θ_d	Angular velocity at touch-down ($\theta_d \times \sqrt{g/l_0}$)	0.69–1.77	2.19–5.64 radian/s
L_d	Radial velocity at touch-down ($L_d \times \sqrt{gl_0}$)	0.15–0.61	0.47–1.94 m/s
$\Delta L_{\max}, \Delta l_{\max}$	Maximum leg spring deflection ($\Delta L_{\max} \times l_0$)	0.04–0.17	0.04–0.18 m
$K_{\text{real}}, k_{\text{real}}$	Leg stiffness ($K_{\text{real}} \times \text{mg}/l_0$)	12–50	8–33 kN/m

The presented data based on the experiment as well as from papers [12, 17, 18, 25]. Additional parameters: initial distance of the center of mass to the ground $l_0 = 1.03$ m, body mass $m = 69$ kg, and gravitational acceleration $g = 9.81\ \text{m/s}^2$. A capital letter indicates a nondimensional parameter, while a lower case letter indicates a dimensional parameter

of the amplitude $B(\epsilon)$ of the radial motion $L(t)$ and the shift $A(\epsilon)$ of the touch-down position, i.e.,

$$\Delta L_{\max} \approx \widetilde{\Delta L}_{\max} := B(\epsilon) - A(\epsilon). \tag{7}$$

For more information we refer to [12, 15].

Since $\theta(0) = \theta_{\mathrm{TD}} = -\alpha$ and $\theta(t_{\mathrm{C}}) = \theta_{\mathrm{TO}} = \beta = \Delta\theta - \alpha$, the second order approximation of the angle swept during stance $\Delta\theta$ is as follows

$$\Delta\theta \approx \widetilde{\Delta\theta}_2 := \pi\theta_d\epsilon + \left[4\theta_d L_d - 2\frac{\theta_d}{L_d}\left(\theta_d^2 - \cos\alpha\right) - \frac{1}{2}\pi^2\sin\alpha\right]\epsilon^2, \quad \text{(the second order)}, \tag{8}$$

where $\epsilon \to 0$ (all terms of the order $O(\epsilon^3)$ in formula (8) are omitted). Moreover, the first order approximation of $\Delta\theta$ (see (8)) is given by

$$\Delta\theta \approx \widetilde{\Delta\theta}_1 := \pi\theta_d\epsilon, \qquad \text{(the first order)}. \tag{9}$$

Solving the equation

$$\widetilde{\Delta\theta}_i = \alpha + \beta, \quad \text{for} \quad i = 1, 2,$$

for the boundary problem of a single support phase. Due to $\sqrt{K} = 1/\epsilon$, where $\widetilde{\Delta\theta}_i$ is given by formula (8) or (9), we get the following two approximations of the leg stiffness K of the second and first order:

$$K \approx \widetilde{K}_2 := \left[\frac{\pi\theta_d + \sqrt{\Delta}}{2(\alpha+\beta)}\right]^2, \qquad \text{(the second order)} \tag{10}$$

with

$$\Delta = \pi^2\theta_d^2 + 8\alpha\left[4\theta_d L_d - 2\frac{\theta_d}{L_d}\left(\theta_d^2 - \cos\alpha\right) - \frac{1}{2}\pi^2\sin\alpha\right], \tag{11}$$

and

$$K \approx \widetilde{K}_1 := \left(\frac{\pi\theta_d}{\alpha+\beta}\right)^2, \qquad \text{(the first order)}. \tag{12}$$

In [26] it is shown that the leading order of the expansion of K as $\alpha \to 0^+$ for the asymptotic solutions (for the symmetric case $\alpha = \beta$) is actually the same as $\widetilde{K}_1$. On the other hand, $\widetilde{K}_2$ can be used to solve an asymmetric boundary problem. If $\alpha + \beta \to 0^+$ then $K \to \infty$ and both approximations of K are very good (cf. [15]). However, for moderately small values of the parameters sum $\alpha + \beta$, $\widetilde{K}_2$ is more accurate than $\widetilde{K}_1$, which was derived assuming small $\Delta\theta$. For Δ to be non-negative (see (11)), the mutual relationship between θ_d and the system energy must be satisfied. It is always valid for jogging speeds, i.e. $\theta_d = \sqrt{\cos\alpha} \approx 1$, but could be also satisfied for the slightly faster runs (see the results in Sect. 3).

An important parameter of running, apart from stiffness, is the mechanical energy of the system. The dimensionless form of the mechanical energy, during contact phase, is given by

$$E_s = \frac{1}{2}\left[(L')^2 + L^2(\theta')^2 + K(1-L)^2\right] + L\cos\theta. \tag{13}$$

By appropriately concatenating asymptotic solutions for the two phases, we are able to reduce the dynamics to the following one-dimensional apex to apex return map (cf. [15])

$$Y_{i+1}(Y_i) = \cos(\Delta\theta - \alpha) + \left[\sin(2\alpha - \Delta\theta)\sqrt{E_s - Y_i} + \cos(2\alpha - \Delta\theta)\sqrt{Y_i - \cos\alpha}\right]^2, \tag{14}$$

where in the ith period the apex height Y_i changes to the apex height Y_{i+1}, and $\Delta\theta$ is given by 8 or 9. Stable and unstable fixed points Y^*, i.e. $Y^* = Y_i = Y_{i+1}$, have been studied in references [12, 15] for symmetrical solutions ($\alpha = \beta$). Theorem 4.1 from reference [15] gives the condition for the existence of symmetric solutions related to the energy on that symmetric periodic solution. The minimum required energy is expressed analytically by

$$E_{\min} = \frac{\left(\theta_d^*\right)^2}{2\cos^2\alpha} + \cos\alpha, \tag{15}$$

where θ_d^* represents the angular velocity θ_d at the fixed point Y^*. In addition, if the system energy slightly exceeds the minimum energy, i.e. $E_s > E_{\min}$ (see Theorem 4.2 from [15]), then the obtained fixed points Y^* for symmetric solutions are stable. To use $E_{\min}$ formula also for asymmetric solutions, the mean of the attack and take-off angles could be substituted into (15):

$$\frac{\left(\theta_d^*\right)^2}{2\cos^2\frac{\alpha+\beta}{2}} + \cos\frac{\alpha+\beta}{2}.$$

A more detailed explanation giving the rationale behind the above formula is given Sect. 2.5.2.

2.2 Participants

One hundred and five healthy, physical education students (gender: 71 males and 34 females; mean ± SD: age 20 ± 3 years, height 175 ± 9 cm, and mass 69 ± 11 kg) voluntarily participated in this study. The group includes some running specialists, representatives of other disciplines, and recreational sports people. The detailed course of the experiment was presented to them, and informed written consent was obtained from the Participants. The study was conducted according to the Declaration of Helsinki. The testing protocol was accepted by the Human Ethics

Committee of the Wroclaw University of Science and Technology and does not require an ethics code.

2.3 Procedure

The study was carried out at the Athlete Movement Biomechanics Laboratory of the University of Rzeszów. After a standardized warm up, including 15-min low-intensity running and stretching of the entire body, the volunteers rested until they gained a total subjective readiness to perform the test. In the main experiment they performed four 15-s tries on a treadmill (h/p/cosmos sports & medical GmbH, Nussdorf-Traunstein, Germany) with different targeted velocities, starting from the slowest to the fastest (9, 12.5, 16, 19.5 km/h, respectively). Each attempt was preceded by increasing the treadmill velocity, to reach the target speed. The time between each trial was a 2 min passive rest. The recovery was used to avoid fatigue effects and to ensure that each trial was performed with maximum physical readiness by a rested participant. Studies have shown that in the depleted muscle all of the adenosine triphosphate (ATP) and phosphocreatine (PCr) are restored within 2 min after an "all-out" bout [27]. During a 15-s submaximal intensity effort, the glycolytic pathway with the waste product lactate (La^-) does not become the major provider of ATP [28]. Therefore, the running mechanics were not disturbed during the trials, see [29, 30].

All testings were performed in preferred form-fitting training clothes that did not restrict movement, including their own shoes. The markers were placed on the lateral surface of the participant's body, on one side opposite the camera. The center of mass (CoM) marker, representing the mass point position, was on the height of the median sacral region, behind S2. It is the landmark of the horizontal projection of the center of body mass (cf. [31]), located, according to [32], at 56% of the runner's total height in a standing position. Certainly, the position of the center of mass depends on individual somatic characteristics and will vary during movement. However, by transitioning to dimensionless variables, the most important aspect from the standpoint of subsequent analysis is to ensure that the marker is located in the same anatomical position for all participants. The second marker was placed on the ankle, at the level of the lateral malleolus of the fibula, as the model ignores the foot movement [33].

2.4 Data collection

At the beginning, initial, radial distance of the center of mass to the ground (l_0) has been measured in a standing position as the length of the segment starting at CoM, passing through second marker and ending at the point of foot contact with the ground (the ball of the foot location).

The running gaits analysis was realized using a Gaitway 3D system from Arsalis (h/p/cosmos sports & medical GmbH, Nussdorf-Traunstein, Germany) based on 4 tensometers equipped with a validated Zebris pressure platform (zebris Medical GmbH, Isny im Allgäu, Germany) located under the running belt [34]. Force was measured at 1000 Hz frequency. As a result, it is known when the foot was in contact with the ground and it was possible to determine the moments of touch-down, take-off and the moment of greatest ground reaction force (GRF).

The athletes were also filmed using two synchronized, high-speed video cameras (Ninox 300c, Noraxon, Scottsdale, USA) at 100 fps. The center of mass and ankle markers were digitized for each frame, creating a simple one-segment model of the athlete. Touch-down and take-off moments, detected from GRF, overlapped the frames where the foot had clear contact with the ground and where the foot had clearly left the ground [33], while the moment when the CoM was closest to the ground fell on the greatest ground reaction force (see [35]). Then the angles of attack and take-off as well as the minimum radial distance of the center of mass to the ground were collected using the SIMI Motion System (SIMI Reality Motion Systems GmbH, Unterschleissheim, Germany). The real dimensions of the recorded image were determined by calibration frame (1×1 m) placed in a plane of the participant's movement. After coordinate calibration, the minimum radial distance from the center of mass to the ground was measured as the distance from the CoM marker to the point of foot contact with the ground.

Additionally, a validated triaxial accelerometer Shimmer 9DOF [36] (, Shimmer Research Ltd, Dublin, Ireland) was placed on the back sacral localization—approximate level of the center of mass in a standing position, (as in [32]) of each participant. The acceleration data were measured with 300 Hz frequency and smoothed by a fourth-order low-pass Butterworth filter with a cut-off frequency of 10 Hz (based on [37, 38]). Referring to the spring mass model, ground contact starts when the vertical component of acceleration crosses zero. What's more, we assume that at the time of the largest GRF, the vertical velocity is zero and the horizontal velocity is equal to the speed of the treadmill. Taking them as initial values for each subsequent step, both velocity components were calculated during touching-down by numerical integration.

2.5 Data analysis

Trials included from 20 to 30 ground contacts. For each ground contact, the amplitude of the active peak of vertical ground reaction force was determined and mean of those

peaks (denoted by f_{max}) was used for final analysis (see Fig. 2a). The horizontal velocities were calculated as the resultant of the speed of the treadmill and the instantaneous pelvis velocity, taken from accelerometers. The vertical velocities of the center of mass were collected from accelerometers data, also at the instants of touch-down (see Fig. 2b). Similarly, both velocities were averaged and denoted by u and v. Finally, the minimum distance of the center of mass to the ground, touch-down and take-off angles (i.e. α, β) were collected from the successive contact phases, and the mean of these parameters was taken for further processing.

Angles were formed by the segment of the center of mass and the ankle markers in relation to the vertical axis (see Fig. 3). The minimum radial distance of the CoM marker to the ground was measured along the path passing through both markers (assuming that the peak CoM downward displacement occurs at the moment f_{max} is reached [35]). Then the maximum displacement of the leg spring Δl_{max}, so the difference between the initial and minimum distance of the center of mass to the ground, was calculated. This parameter is characterized by the greatest measurement error, as even small differences in the calibration may significantly affect the result.

The collected data are presented in Table 2. Additionally, Table 2 contains information obtained from the pressure plate, i.e. mean time of foot contact with the ground (t_c), as well as mean time of the flight phase (t_a) and step frequency. Then the values presented in Table 2 were converted into dimensionless quantities and further used for comparisons.

2.5.1 Leg stiffness

The real and dimensional value of the leg spring stiffness, denoted by k_{real}, was calculated as follows:

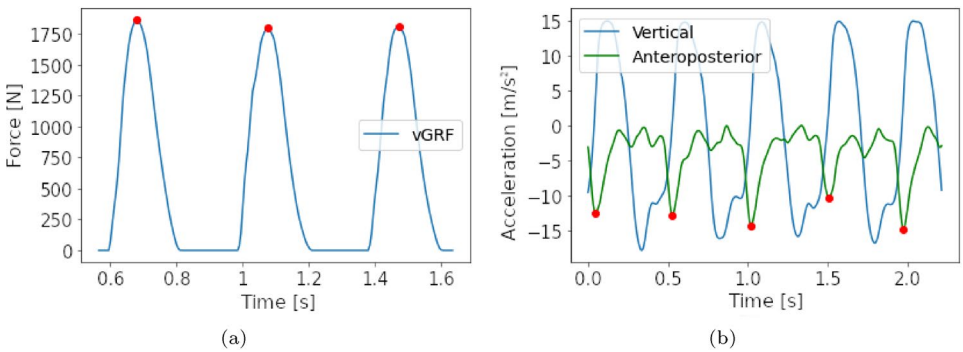

Fig. 2 An example of: **a** vertical ground reaction force (denoted by vGRF) with active peaks marked with red circles. **b** Filtered vertical and anteroposterior sacral acceleration data, relative to the device's local coordinate system, with touch-down moments marked with red circles

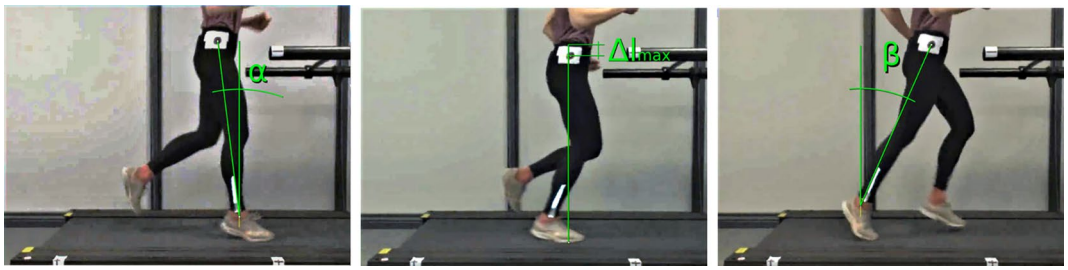

Fig. 3 Touch-down and take-off angles α, β and minimum distance from the center of mass to the ground assessment

Table 2 Mean of the collected data for the running parameters: α, β, u, v, Δl_{max}, f_{max}, t_c, t_a, and the step frequency in the last column, depending on the speed

Speed (km/h)	α (°)	β (°)	u (m/s)	v (m/s)	Δl_{max} (m)	f_{max} (kN)	t_c (s)	t_a (s)	(step/s)
9	5.59	24.27	2.5−0.074	−0.476	0.017	1.435	0.30	0.08	2.69
12.5	8.05	25.47	3.5−0.074	−0.457	0.017	1.512	0.24	0.10	2.96
16	9.67	27.73	4.4−0.119	−0.419	0.021	1.517	0.20	0.11	3.20
19.5	10.40	28.95	5.4−0.126	−0.378	0.019	1.528	0.18	0.15	3.03

The horizontal velocity u is the vector sum of the treadmill speed and the velocity of the CoM obtained directly from the accelerometer. All parameter values are dimensional

$$k_{\text{real}} = \frac{f_{\max}}{\Delta l_{\max}}, \tag{16}$$

and recalculated to the dimensionless value K_{real}, multiplied by $\frac{l_0}{mg}$ (see (2) and Table 1). The observed runs were stable i.e. running parameters repeated and, because of short tries duration, the fatigue did not cause any changes in gait characteristics (see [39]). Therefore, we could use the leg stiffness approximation formulas: $\widetilde{K}_1$ and $\widetilde{K}_2$, for the boundary problem calculated from Eqs. (10) and (12), respectively. The comparison between the calculated values of leg stiffness using both methods and the real values was evaluated using a dependent t test. The variations in the parameters of $\widetilde{K}_1$, $\widetilde{K}_2$ and $\widetilde{K}_{\text{real}}$ across the four velocities were determined through repeated measurements and a one-way analysis of variance (ANOVA) with a post-hoc Tukey test. The level of significance was set at 0.05.

2.5.2 Energy

We want to assess whether the mechanical energy during running is optimized. To this aim we require some reference point with respect to which such an optimum value may be established, and this reference is provided by the model. We have to bear in mind though that the mechanical energy of the model system was calculated using formula (13) and the minimum energy is given by Eq. (15), which applies when there is an angular symmetry between landing and take off. In other words, when both angles are the same. However, as already mentioned, when athletes are observed during running, there is a clear angular asymmetry between the landing (α) and take off angles (β), but there is no significant asymmetry in the vertical height of the center of mass at these instances. To be able to still apply our model system as an analytical reference point, we use this observation. That is, even though β angle is larger than α, runners land on their bent knee and the radial distance from the center of mass to the point of contact with the ground is less than l_0. Therefore, it is possible that the center of mass during take off and touchdown are on the same level (cf. [40]). Hence, there is still symmetry in the system, and we assume angle α used in formula (15) to be the arithmetic mean of angles α and β.

3 Results

Approximations related to the stiffness of the leg: maximum leg deflection ($\Delta L_{\max}$), contact time (T_c) and angle swept $\Delta\theta$, and their equivalents derived directly from experimental data, are presented in the Fig. 4 below.

The dimensionless maximum leg spring deflection, i.e. $\Delta L_{\max} = \Delta l_{\max}/l_0$, is about 0.04 smaller than the approximation $\widetilde{\Delta L}_{\max}$ (see Fig. 4 on the left). The real contact time of the foot with the ground after normalization is greater than the $\widetilde{T}_c$ value by about 0.02 (see Fig. 4 inside). The $\widetilde{\Delta\theta}_2$ (see Fig. 4 on the right) differs by up to 4° from the actual value of $\Delta\theta = \alpha + \beta$. It also exhibits an increasing trend with rising speed.

It turns out that for the fastest runs, i.e. 19.5 km/h, only in 6 cases out of 105 the set of parameters did not allow the calculation of the $\widetilde{K}_2$ approximation, see Eq. (10), because Δ was negative, see Eq. (11). With slower runs the calculation of $\widetilde{K}_2$ approximation posed no problems, because for small θ_d, the second factor in (11) is positive. With increasing speed, the real leg stiffness remained unchanged, while $\widetilde{K}_1$ significantly increased and $\widetilde{K}_2$ decreased, see Fig. 5. A statistically significant difference (p value < 0.05) between the real values of leg spring stiffness and first-order approximation $\widetilde{K}_1$, has not been observed only for lowest velocity, while $\widetilde{K}_1$ and K_{real} had statistically significantly different values for all other velocities. Therefore, we will use a more accurate second-order approximation (8) in the mapping construction.

Energy E_s (see (13)) and the minimum energy needed for stable running $E_{\min}$ (see (15)) are increasing with increasing running speed (see Table 3). They have similar values, and $E_{\min}$ is only slightly smaller than E_s.

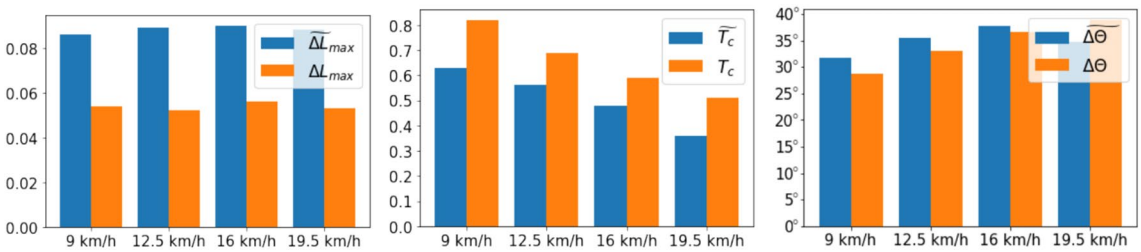

Fig. 4 Comparison of the nondimensional, mean values of approximations $\widetilde{\Delta L}_{\max}$, $\widetilde{T}_c$ and $\widetilde{\Delta\theta}_2$, given by formulas (7), (5) and (8), respectively, with the mean values of the experimental data for these running parameters (measured and appropriately normalized). The means were calculated for the sample of $n = 105$ runners

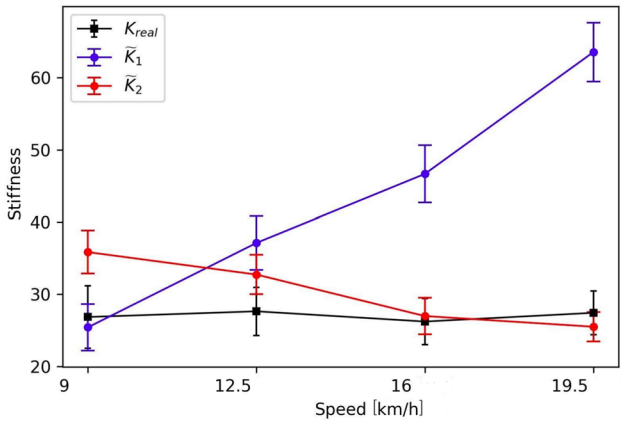

Fig. 5 Comparison of the leg spring stiffness, denoted by K_{real}, and both approximations $\widetilde{K}_1$ and $\widetilde{K}_2$, calculated from formulas (12) and (10), respectively, for the four running speeds. Additionally, plus and minus the sample standard deviation are plotted

Table 3 The mean value of system's energy E_s on a periodic solution (see Eq. (13)) and minimum energy required for stable running $E_{\min}$ (see Eq. (15)) depending on the running speed

Speed (km/h)	$E_s \pm$ SD	$E_{\min} \pm$ SD
9	1.14 ± 0.037	1.11 ± 0.033
12.5	1.37 ± 0.075	1.33 ± 0.081
16	1.66 ± 0.106	1.62 ± 0.110
19.5	2.13 ± 0.143	2.12 ± 0.158

Additionally, ± SD is determined for each column, which is plus or minus the sample standard deviation

4 Discussion

The main findings of this study were the observation that humans run with the minimum energy required for stable running. This thesis was proven using the SLIP model as a reference point for the mechanical properties and energetics of human running gaits. An important step, in this process, was to verify the spring-mass model by combining experimental data with leg stiffness approximations. There are many models of gait and running in the literature. The musculoskeletal model [41], a biometric model [42, 43], a SLIP model [11, 12], and a dynamic model [44], but their values are not calculated using experimental data. Therefore, we can only refer to values of leg stiffness determined in other papers [8, 18, 20, 45], using ground reaction forces and displacement of the center of mass, with K_{real} from this article.

The relationships between step frequency and leg stiffness were studied in [46]. In other papers was clearly demonstrated that leg stiffness did not significantly change with running speed [17, 19, 20, 35, 47]. It did change though when step frequency varied at a given constant speed. According to [48], step frequency appears to be an indirect factor influencing leg stiffness through its effect on contact time. In our experiment, increasing the speed of the treadmill forces a larger stride frequency. The angle swept during the stance phase also grows, what is typical for runs with low and medium velocities [11, 49], resulting in an increase in spring deflection $\Delta L_{\max}$. Overall the stiffness of the leg remains constant and range between 26.22 ± 3.19 and 27.64 ± 3.34 at velocities from 9 to 19.5 km/h (similar as in [17, 20, 35]). Most of these values are lower than those obtained from both approximations. The main reason may be the difference in the maximum leg deflection ($\Delta L_{\max}$ and $\widetilde{\Delta L}_{\max}$). This may be due to fluctuations resulting from the calibration and the construction of the approximations for the stiffness parameter itself, which is directly independent of $F_{\max}$ and $\Delta L_{\max}$. The values of the second-order approximation are much closer to K_{real} except for the slowest velocity. We should also mention here that Eq. (12), for leg stiffness approximation $\widetilde{K}_1$, is proportional to θ_d squared, and inversely proportional to $\alpha + \beta$ squared. Lower velocities correspond to smaller angles $\alpha + \beta$. For these velocities, based on experimental data, we observe that the stiffness is equal (with statistical significance) to the square of the ratio of θ_d by $\alpha + \beta$ times π. This is not the case for higher velocities. That is, for higher velocities θ_d must vary faster than $\alpha + \beta$, which is the case when $\widetilde{K}_2$ approximation (10) is taken into account. For lower velocities the ratio $\theta_d/(\alpha + \beta)$ is constant, whereas for larger velocities it is the ratio $C\theta_d^{3/2}/(\alpha + \beta)$, which is constant, with C some coefficient. We do not have any evidence that there is some systematic error in the measurements of the take-off and landing angles, that would create the observed effects of the change in the stiffness approximations at different velocities discussed in this paragraph.

Running energetics was analyzed in previous studies. An energy-saving mechanism was observed, using e.g., oxygen consumption [50–52] or another mathematical model for comparison with real parameters [53]. Hence presented results, based on purely mechanical properties of our reduced model system, confirm previous studies suggesting the existence of an optimization mechanism of runners.

The current study has some potential limitations. An obvious limitation is the approximations made in the model and the assumptions, such as the requirement on small angles. This assumption is easily justifiable from the practical point of view for low speeds. As it can be seen in Fig. 5, for low speeds our approximate values of the stiffness parameter are good. However, with kinetic data (velocities of the CoM) and information on the angles of attack and take-off, it is suggested to use the second-order approximation to estimate the stiffness of runner's leg.

In terms of further research, we believe that it would be of interest to determine, and then use in the modeling process, the correlation of running energetics with attack angle α (without considering K), which would facilitate the use of the model in training conditions. This would allow one to investigate, for example, running optimization in terms of fatigue. We posit that the implementation of our proposed methodology has the potential to enhance the quantification of the mechanics of running, specifically with regards to parameters such as stiffness and mechanical energy. Future studies should further explore these aspects to provide more detailed and valuable information on this topic.

5 Conclusions

The runner's mechanical energy was sufficient, but only slightly higher than required minimal energy by the model for stable running. It may be concluded that the runner wants to achieve stability with minimal mechanical energy expenditure. This is an important conclusion of this paper not only in biomechanical or physiological terms, but it also confirms the legitimacy and need for the mathematical models of running. The models are a reference point for the measured parameters, and thanks to them it is known that, for example, in our case, the energy is minimized. However, it is worth bearing in mind that CoM symmetry is different from angular symmetry. It remains the subject of further analytical study to investigate how the analytical approach we apply here is related to the condition on the minimum energy for asymmetric solutions, where asymmetry reflects that the take-off and touch-down angles are different. In our current study, we circumvent this issue by introducing a virtual small angle, which is an arithmetic mean of the attack and take-off angles.

Data availability Data cannot be shared publicly because of concerns over the risk of inadvertent disclosure of adolescent athletes' personal health information and performance information. Data are available from the first author (contact via e-m: zofia.wroblewska@pwr.edu.pl) for researchers who meet the criteria for access to confidential data. In order to proceed with permission to use the data set, it is necessary to conduct a joint investigation with the research staff.

Declarations

Conflict of interest The authors declare no competing of interest. The study did not involve any commercial interest in any of the concepts discussed in the article.

References

1. Folland JP, Allen SAMJ, Black MI, Handsaker JC, Forrester SE (2017) Running technique is an important component of running economy and performance. Med Sci Sports Exerc 49(7):1412–1423
2. Rocco DM, Merni F (2014) The concurrent effects of strike pattern and ground-contact time on running economy. J Sci Med Sport 17(4):414–418
3. Fadillioglu C, Möhler F, Reuter M, Stein T (2022) Changes in key biomechanical parameters according to the expertise level in runners at different running speeds. Bioengineering (Basel) 9(11):616
4. Miyashiro K, Nagahara R, Yamamoto K, Nishijima T (2019) Kinematics of maximal speed sprinting with different running speed, leg length, and step characteristics. Front Sports Active Living 1:37
5. Horst-Moritz M, Shai R, John G, Christian L, Johann R, Andre S (2015) Constructing predictive models of human running. J R Soc Interface 12(103):20140899
6. Oeveren BT, Ruiter CJ, Beek PJ, Dieën JH (2021) The biomechanics of running and running styles: a synthesis. Sports Biomech 4:1–39
7. Donelan JM, Kram R (2000) Exploring dynamic similarity in human running using simulated reduced gravity. J Exp Biol 203(16):2405–2415
8. Bullimore SR, Burn JF (2007) Ability of the planar spring-mass model to predict mechanical parameters in running humans. J Theor Biol 248:686–695
9. Morin J-B, Tomazin K, Edouard P, Millet GY (2011) Changes in running mechanics and spring-mass behavior induced by a mountain ultra-marathon race. J Biomech 44(6):1104–1107
10. Girard O, Micallef J-P, Millet GP (2011) Changes in spring-mass model characteristics during repeated running sprints. Eur J Appl Physiol 111(1):125–134
11. Seyfarth A, Geyer H, Günther M, Blickhan R (2002) A movement criterion for running. J Biomech 35:649–655
12. Geyer H, Seyfarth A, Blickhan R (2005) Spring-mass running: simple approximate solution and application to gait stability. J Theor Biol 232:315–328
13. Burns GT, Gonzalez R, Ronald ZF (2021) Improving spring-mass parameter estimation in running using nonlinear regression methods. J Exp Biol 224(Pt 6):232850
14. Burns GT, Tam N, Santos-Concejero J, Tucker R, Zernicke RF (2023) Assessing spring-mass similarity in elite and recreational runners. Front Physiol 14:1224459
15. Wróblewska Z, Kowalczyk P, Płociniczak Ł (2023) Stability of fixed points in an approximate solution of the spring-mass running model. IMA J Appl Math 83:1–26
16. Blickhan R (1989) The spring-mass model for running and hopping. J Biomech 22(11/12):1217–1227 (**PMC2625422**)
17. McMahon TA, Cheng GC (1990) The mechanics of running: how does stiffness couple with speed? J Biomech 23(1):65–78

18. Arampatzis A, Brüggemann G-P, Metzler V (1999) The effect of speed on leg stiffness and joint kinetics in human running. J Biomech 32:1349–1353
19. Farley CT, González O (1996) Leg stiffness and stride frequency in human running. J Biomech 29(2):181–186
20. Morin J-B, Dalleau G, Kyröläinen H, Jeannin T, Belli A (2005) A simple method for measuring stiffness during running. J Appl Biomech 21:167–180
21. Płociniczak Ł, Wróblewska Z (2020) Solution and asymptotic analysis of a boundary value problem in the spring-mass model of running. Nonlinear Dyn 99:2693–2705
22. Maloney SJ, Fletcher IM (2021) Lower limb stiffness testing in athletic performance: a critical review. Sports Biomech 20:109–130
23. Alessandro G, Mickle MJ, Patric M, Simon TB (2022) Insight into the hierarchical control governing leg stiffness during the stance phase of running. Sci Rep 12:12123
24. Diego J-C, Roche-Seruendo LE, Felton L, Cartón-Llorente A, García-Pinillos F (2021) Stiffness in running: a narrative integrative review. Strength Cond J 43(2):104–115
25. Wróblewska Z (2020) Approximate solutions and numerical analysis of a spring-mass running model. Math Appl 48(1):25–48
26. Okrasińska-Płociniczak H, Płociniczak Ł (2020) Asymptotic solution of a boundary value problem for a spring-mass model of legged locomotion. J Nonlinear Sci 30:2971–2988
27. Bogdanis GC, Nevill ME, Lakomy HK, Boobis LH (1998) Power output and muscle metabolism during and following recovery from 10 and 20 s of maximal sprint exercise in humans. Acta Physiol Scand 163(3):261–272
28. Baker JS, McCormick MC, Robergs RA (2010) Interaction among skeletal muscle metabolic energy systems during intense exercise. J Nutr Metab 2010:905612
29. Belcic I, Rodić S, Dukarić V, Rupčić T, Knjaz D (2021) Do blood lactate levels affect the kinematic patterns of jump shots in handball? Int J Environ Res Public Health 18(20):10809
30. Bernans E (2023) Assessing changes in running kinematics at different intensities: a case study. J Phys Educ Sport 23(5):157–12791286
31. Fazio P, Granieri G, Casetta I, Cesnik E, Mazzacane S, Caliandro P, Pedrielli F, Granieri E (2012) Gait measures with a triaxial accelerometer among patients with neurological impairment. Neurol Sci 34(4):435–440
32. Davidovits P (2018) Physics in biology and medicine, 5th ed. Academic Press: London.
33. Gustafsson M, Zarnblom D (2015) Determination of biomechanical key parameters in women's long jump - Ananalysis of Swedish elite athletes in a competitive setting. Doctoral dissertation. University of Gothenburg, Sweden. Available at Gothenburg University Library Campus Repository:https://gupea.ub.gu.se/handle/2077/40067. Accessed 12 Jun 2024.
34. Van Alsenoy K, Thomson A, Burnett A (2019) Reliability and validity of the zebris fdm-thq instrumented treadmill during running trials. Sports Biomech 18(5):501–514
35. Morin J-B, Jeannin T, Chevallier B, Belli A (2006) Spring-mass model characteristics during sprint running: correlation with performance and fatigue-induced changes. Orthop Biomech 27(2):158–165
36. Shafi J, Krishna PV (2020) Detecting accuracy of accelerometer and gyroscope wearable shimmer sensors using linear regression. Int J Recent Technol Eng (IJRTE) 8(5):1992–1998
37. Crenna F, Battista Rossi G, Berardengo M (2021) Filtering biomechanical signals in movement analysis. Sensors 21:4858
38. Day EM, Alcantara RS, McGeehan MA, Grabowski AM, Hahn ME (2021) Low-pass filter cutoff frequency affects sacral-mounted inertial measurement unit estimations of peak vertical ground reaction force and contact time during treadmill running. J Biomech 119:110323
39. García-Pinillos F, Cartón-Llorente A, Jaén-Carrillo D, Delgado-Floody P, Carrasco-Alarcóna V, Martínez C, Roche-Seruendo LE (2020) Does fatigue alter step characteristics and stiffness during running? Gait Posture 76:259–263
40. Lussiana T, Patoz A, Gindre C, Mourot L, Hébert-Losier K (2019) The implications of time on the ground on running economy: less is not always better. J Exp Biol 222(6):192047
41. Wang Y, Li X, Huang P, Li G, Fang P (2018) An analysis of biomechanical characteristics of gait based on the musculoskeletal model. In: 2018 IEEE international conference on cyborg and bionic systems (CBS), Shenzhen, China, pp 151–154
42. Yam C-Y, Nixon MS, Carter JN (2001) Extended model-based automatic gait recognition of walking and running. In: Lecture Notes in Computer Science, vol. 2091. Springer. First Online: 01 January 2001
43. Yam C, Nixon MS, Carter JN (2004) Automated person recognition by walking and running via model-based approaches. Pattern Recognit 37(5):1057–1072
44. Amos A, Gerth W (2003) Analytic path planning algorithms for bipedal robots without a trunk. J Intell Robot Syst 36(2):109–127
45. Brughelli M, Cronin J (2008) Influence of running velocity on vertical, leg and joint stiffness. Sports Med 8(38):647–657
46. Farley CT, Glasheen J, McMahon TA (1993) Running springs: speed and animal size. J Exp Biol 185(1):71–86
47. He JP, Kram R, McMahon TA (1991) Mechanics of running under simulated gravity. J Appl Physiol 71(3):863–870
48. Morin J-B, Samozino P, Zameziati K, Belli A (2007) Effects of altered stride frequency and contact time on leg-spring behavior in human running. J Biomech 40:3341–3348
49. Hay JG (1973) The biomechanics of sports techniques. Prentice-Hall, Inc.: Englewood cliffs, N.J.
50. Cavanagh PR, Williams KR (1982) The effect of stride length variation on oxygen uptake during distance running. Med Sci Sports Exerc 14(1):30–35
51. Moore IS, Jones AM, Dixon SJ (2012) Mechanisms for improved running economy in beginner runners. Med Sci Sports Exerc 44(9):1756–1763
52. Ruiter CJ, Verdijk PWL, Werker W, Zuidema MJ, Haan A (2014) Stride frequency in relation to oxygen consumption in experienced and novice runners. Eur J Sport Sci 14(3):251–258
53. Moore IS, Ashford KJ, Cross C, Hope J, Jones HSR, McCarthy-Ryan M (2019) Humans optimize ground contact time and leg stiffness to minimize the metabolic cost of running. Front Sports Act Living 1:53